



## Examining phase response curve of nerve cell by using three different methods

Hasan ESKALEN<sup>1</sup>, Şükrü ÖZĞAN<sup>2,\*</sup>

<sup>1</sup>Bioengineering Program, Graduate School of Natural and Applied Science, Kahramanmaraş Sütçü İmam University, 46040, Kahramanmaraş, Turkey

<sup>2</sup>Department of Physics, Faculty of Arts and Sciences, Kahramanmaraş Sütçü İmam University, 46040, Kahramanmaraş, Turkey

Received: 13September 2017, Revised: 27 November 2017, Accepted: 05 December 2017

\*Corresponding author's e-mail address: ozgans@gmail.com (Ş. Özğan)

### ABSTRACT

Rhythmic motion is observed in a variety of different field including physical, chemical and biological systems. Neural system, that consists of billions of neurons are also exhibited periodic motion. Phase Response Curves (PRCs); act like a bridge between, a single neuron and neural network; briefly measure change in period of oscillation by giving perturbation at different points of oscillation. PRCs can determined from measurements of electrical activities of neurons by experimental methods or theoretically derived from three different methods. As far as we know from the literature, these three different methods have never been used at the same time before. The main purpose of this computational study is to the obtain Phase Response Curve by three different methods and compare them in terms of simulation times and peak to baseline ratio. First, the kinds of excitability of neurons, the types of Phase Response Curve and peak to baseline ratio are mentioned. After then, these three different methods to obtain PRC are explained deeply. At a final step, Phase Response Curves are obtained from three theoretical methods and compared regarding to peak to baseline ratio, simulation time and applicability.

**Keywords:** Phase response curve, direct method, linear adjoint method, adapted direct method.

### Üç farklı metot kullanarak sinir hücrelerinin faz resetleme eğrilerinin incelenmesi

#### ÖZ

Ritmik hareket fiziksel, kimyasal ve biyolojik sistemleri ihtiva eden farklı alanların birçoğunda görülmektedir. Milyarlarca nöronlardan oluşan sinir sistemi periyodik hareket sergilemektedir. Faz Resetleme Eğrileri (PRCs), tek bir nöron ve nöron ağı arasında bir köprü gibi rol oynar ve kısaca farklı salınım noktalarında verilen uyarıcılar ile salınım periyodundaki değişimi ölçer. PRC'ler deneysel olarak nöronların elektriksel aktivitelerinin ölçümlerinden ya da teorik olarak türetilen üç farklı metottan hesaplanabilir. Literatürden bildiğimiz kadarıyla bu üç farklı teorik metot daha önce aynı anda hiç kullanılmamıştır. Bu hesaplamalı çalışmanın ana amacı üç farklı metot ile Faz Cevap Eğrilerini teorik olarak elde etmektir ve onları simülasyon süreleri ve tavan-taban oranları açısından kıyaslamaktır. İlk olarak nöronların uyarılabilirlik çeşitleri, PRC'lerin çeşitleri ve tavan-taban oranı bahsedilmiştir. Daha sonra PRC elde etmekte kullanılan üç farklı metot açıklanmıştır. Son aşamada üç teorik metotla Faz Resetleme Eğrileri türetilmiştir ve elde edilen şekiller tavan-taban oranı, simülasyon süresi ve uygulanabilirliği açısından karşılaştırılmıştır.

**Anahtar Kelimeler:** Faz tepki eğrisi, direkt metot, lineer adjoint metot, uyarlanmış direkt metot.

### 1. INTRODUCTION

Oscillating systems is in everywhere we encounter without realizing in everyday life. Some examples of oscillating systems from biology, chemistry, physics and engineering are single nerve cell that generates action potential<sup>1-4</sup>, heart beat rhythm<sup>5,6</sup>, human walking motion<sup>7,8</sup>, circadian clock<sup>9,10</sup>, oscillation in chemical reactions<sup>11,12</sup> and earthquake dynamics.<sup>13</sup> In short,

systems with dynamical elements that compose of spontaneous rhythms are used for Phase Response Curves (PRCs).<sup>14</sup>

Self-sustained oscillators have been proposed firstly by Andronov and Vitt in 1937 and are one of the areas that are of interest in the researchers working on dynamic systems. The most important feature of the self-sustained release is that it continues to oscillate with its own rhythm when abstracted from the environment.<sup>15</sup> In a

clearer sense, they continue to oscillate without exerting a force on the system. Self-sustained oscillations can be represented geometrically by a stable limit cycle.<sup>16</sup> The stable limit cycles are stable against small amplitude external forces. The oscillating systems do not occur if the limit cycle does not occur, and so PRC cannot be mentioned.<sup>17</sup>

Neurons are the basic operators and information-carrying units of the central nervous system. A single neuron cell emits periodically spikes when the externally applied current value rises above a certain threshold value, and the frequency of spikes increases with increasing amplitude of the applied current.<sup>18,19</sup> Nerve cells at different points of the brain come together with complicated connections and emit spikes synchronously. This mechanism forms basis of fundamental physiological functions of the human such as attention and short-term memory.<sup>17,20</sup> Although synchronous rhythm is a key specification of the human nerve system, the decreasing abnormal synchrony can cause Schizophrenia<sup>21-23</sup> and Alzheimer<sup>24,25</sup>, and the increasing abnormal synchrony can also lead Parkinson<sup>26-28</sup> and Epilepsy.<sup>29,30</sup> These neurodegenerative diseases have also attracted the attention of the scientists that focus on biotechnological studies. Moreover, some institutes consider computational neuroscience as a subtopic of biotechnology. Phase response curve for 24-hour day rhythms is named as circadian clock. The scientists have won the Nobel Prize of 2017 year in physiology and medicine for their discovery of molecular mechanism controlling circadian rhythm.<sup>31</sup> For these reasons, it is very important to examine the PRCs which is related to a single neuron cell, the behaviour of the neuron network, and circadian rhythm.

The PRC is one of the most important tools for investigating the dynamic structure of neurons. In the self-sustaining oscillation, the period of oscillating system dividing equally spaced phases according to a particular reference point and PRC measures how small perturbation given in different phases change the period of oscillations. The shape of PRC provides invaluable information about excitability of neurons, oscillation stability and synchrony in the neural network.<sup>32-38</sup> Shape of PRCs can be obtained from two different fundamental methods. The first method (i.e. experimental method) is the measurement of electro-activity of nerve cells.<sup>39-46</sup> The second method is to calculate PRC theoretically. To best of our knowledge, there are only three different theoretical ways to derive PRC and these three main ways have not been examined together.

In this study, firstly the types of excitability of neurons are examined and then peak to baseline ratio is investigated. Direct method, linear adjoint method and adapted direct method are examined in shortly. PRC of single neuron calculated by using these three different methods, their required time interval, and peak to base line ratios are compared.

## 2. MODEL AND METHODS

In our study,  $I_{Na,p} + I_K$  model is used to simulate the neuron. This model is consist of sodium, potassium and leak current and it is similar to Morris Lecar model.<sup>2</sup>  $I_{Na,p} + I_K$  model is represented by two nonlinear differential equations and it is considered as a simplified version of Hodgkin Huxley model. Nowadays, Hodgkin Huxley type models are known as conductance-based models. In all conductance-based models, the electrochemical processes at the current generation and signal transmission in a neuron are replaced by a facilitated electrical circuit.<sup>47</sup> Equations of the models are:

$$C \frac{dV}{dt} = I_{app} - g_L(V - E_L) - g_{Na}m_{\infty}(V)(V - E_{Na}) - g_K n(V - E_K) \quad (1a)$$

$$dn/dt = (n_{\infty}(V) - n)/(tau(V)) \quad (1b)$$

In Eq. (1a),  $I_{app}$  implies external applied current and  $C$  represents membrane capacitance. The conductance values of sodium, potassium and leak currents,  $g_{Na} = 20$ ,  $g_K = 10$ ,  $g_L = 8$  nS, respectively. The reversal potentials of sodium and potassium are 60 mV and -90 mV. In Eq. (1b), the numerical value of  $tau(V)$  is equal to one. The values of  $m_{\infty}(V)$  and  $n_{\infty}(V)$  are calculated from Eq. (2),

$$x_{\infty}(V) = 1/1 + \exp\{(V_{1/2} - V)/k\}; \quad x = m, n \quad (2)$$

Parameters obtained for different types of excitabilities are given in Table 1.

**Table 1.** Some parameters of  $I_{Na,p} + I_K$  model with different excitability

	Type-1 excitability		Type-2 excitability	
	$k$	$V_{1/2}$	$k$	$V_{1/2}$
$m_{\infty}(V)$	15	-20 (mV)	15	-20 (mV)
$n_{\infty}(V)$	5	-25 (mV)	5	-45 (mV)
$E_L$		-80		-78

The model equations and model parameters are obtained from Izhikevich's book.<sup>2</sup> In this paper, all simulations were performed using a personal laptop, with 10.0 GB RAM and 2.4 GHz Intel i5 processor. Moreover, solutions of differential equations were performed by using the ode45 function (implements fourth order Runge-Kutta numerical integration algorithms) in MATLAB software (R2012b) on a 64-bit mac osx operation systems.

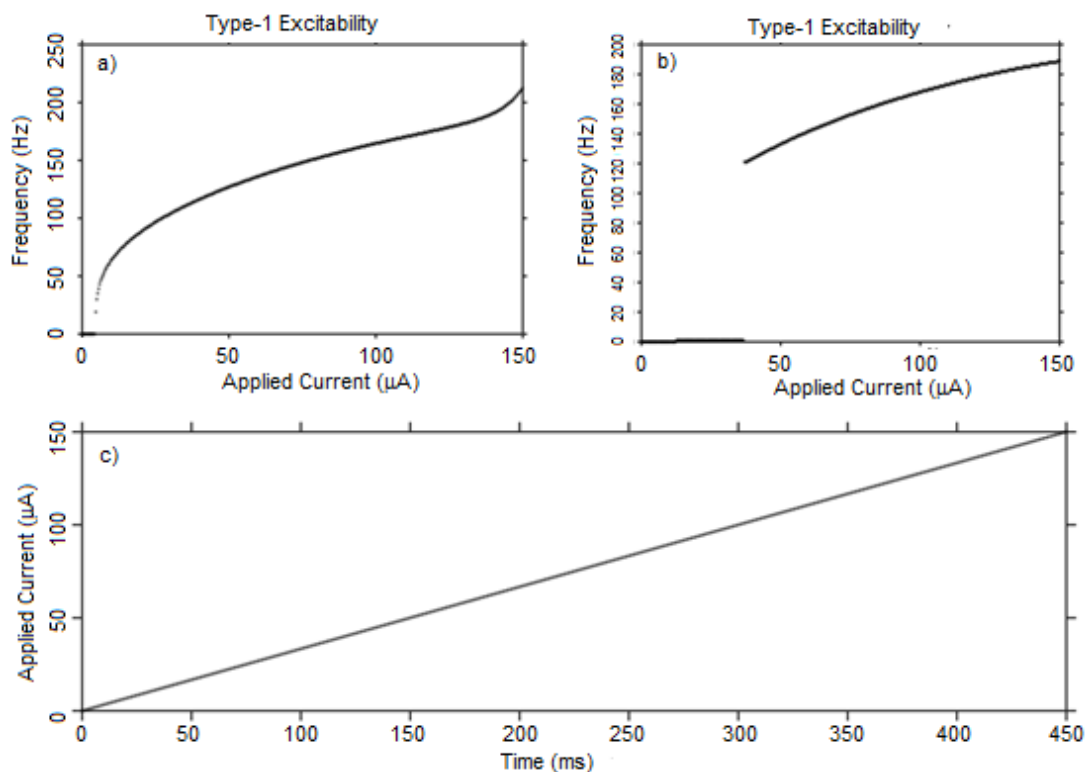


**Figure 1.** The types of excitation derived from the  $I_{Na,p} + I_K$  model and the applied current: a) Excitability Type-1, b) Excitability Type-2, c) Change of applied current with time.

## 2.1. Types of excitability

Nerve cells were stimulated under different voltages applied by using,  $I_{Na,p} + I_K$  model, and the obtained parameters are given in Table 1. The frequencies versus currents applied are plotted in Figure 1. The nerve cell first time emits spike before the applied current reaches 5 pA and as the applied current increases, the spike frequency also increases. This type of excitability is known as Type-1 Excitability<sup>48,49</sup> and it is shown in Figure 1a. On the other hand, if the nerve cell does not emit spikes linearly with the applied currents and the frequency and applied current are relatively high when the nerve cell first time emits spike in Type-2 Excitability.<sup>50</sup> Figure 1b illustrates Type-2 Excitability.<sup>50</sup> Applied current is increased linearly with simulation time and it is given in Figure 1c. To sum up, as indicated in Table 1, the excitability of  $I_{Na,p} + I_K$  model changes with only changing values of two parameters that are  $V_{1/2}$  and  $E_L$ .

## 2.2. Types of PRCs

Excitability types of  $I_{Na,p} + I_K$  model by using parameters in Table 1 and their corresponding PRC types are shown in Figure 2. Generally, Type-1 PRC has an

either positive or negative single curve, but Type-2 PRC is represented by both the combination of positive and negative parts. The Type-1 and Type-2 PRCs are illustrated in Figures 2a and 2b, respectively.

## 2.3. Peak-to-baseline ratio

Peak-to-baseline ratio is applicable for only Type-2 PRCs and it is given by Eq. (3)<sup>51</sup>,

$$r = \frac{|m_l - m_e|}{|m_l + m_e|} \quad (3)$$

At Eq. (3),  $r$  implies peak-to-baseline ratio,  $m_e$  and  $m_l$  represent early and late peak amplitude of PRC. Since Type-2 PRCs are composed of two different sign peaks,  $m_e$  and  $m_l$  are opposite signs. The magnitude of  $m_e$  and  $m_l$  could be easily found from PRC curve.<sup>52</sup> The general shape of Type-2 PRC is given in Figure 3a. The corresponding PRC value of early peak is positive and the late peak is negative. The shape of Type-2 PRC in Figure 3a is derived from  $I_{Na,p} + I_K$  model, and the early (first) peak is positive and it is represented by  $m_e$ .

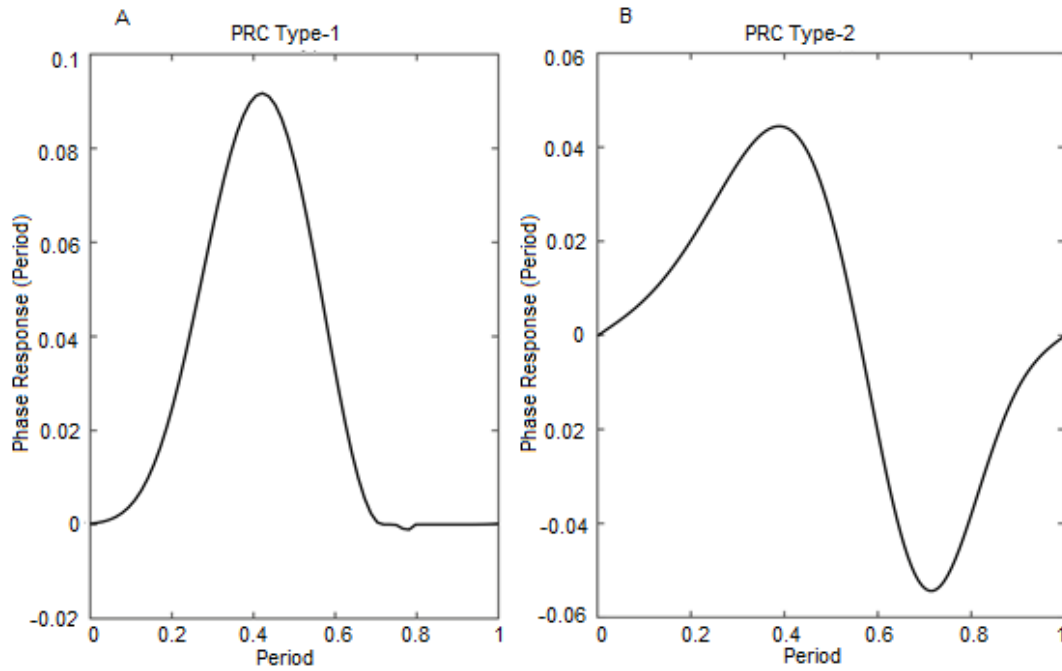


Figure 2. PRC types of  $I_{Na,p} + I_K$  model: a) PRC Type-1, b) PRC Type-2.

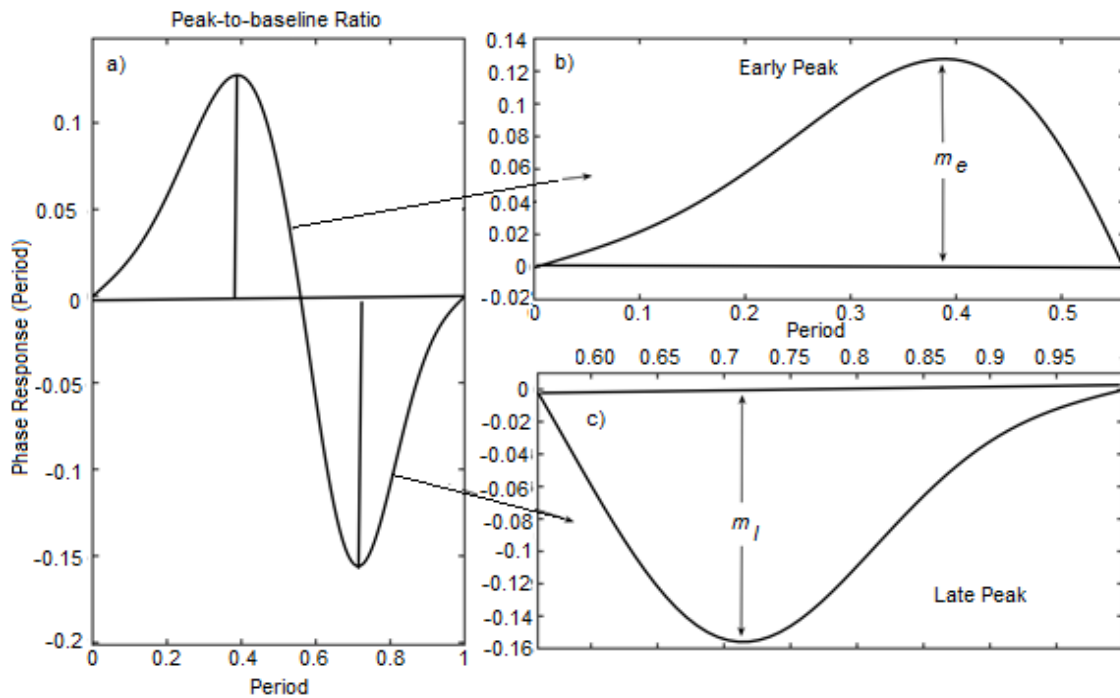


Figure 3. a) Peak-to-Baseline Ratio of PRC Tip-2, b) The first peak of PRC, c) The second peak of PRC.

The late peak is negative and it is represented by  $m_l$ . The early peak is illustrated in Figure 3b and the late peak is shown in Figure 3c.

In this study, phase response curves of  $I_{Na,p} + I_K$  model are theoretically calculated by using three different methods and their simulation times and peak-to-

baseline ratios are calculated. Direct method, linear adjoint methods and adapted direct method are the used methods. To best of our knowledge, these three different methods have not been used and compared together, so far.

## 2.4. Direct method

Suppose the period of self-sustained oscillation is equal to  $T$  and the period of the oscillation after the short perturbation is equal to  $T'$ . The PRC can be calculated with direct method by using Eq. (4),

$$PRC = \frac{T-T'}{T} \quad (4)$$

The first step to find PRC by using direct method is to stimulate self-sustained oscillation for long enough to find initial condition independent solution, i.e. to find limit cycle solution. After then, the time interval for one period oscillation is found, and this period is divided into certain points. Voltage and gating variable values for these certain points are determined. The short perturbation is given to this oscillating system and their voltage and gating variables are found. By using these variable corresponding period points determined. By using time difference between oscillations before and after perturbation, phase response values of one point is obtained and also by giving perturbation at different point of oscillation, phase response curve is obtained.

Figure 4a illustrates voltage versus time graph of  $I_{Na,p} + I_K$  model. The small amplitude, 6 pA, perturbation current is given at 28<sup>th</sup>ms during 0.5 ms. The magnitude of perturbation is 0 pA other than 28<sup>th</sup> ms, this red colored current perturbation curve is given at the voltage axis to only more clearly show the time of the perturbation (Figure 4a). Although the model emits spike periodically before perturbation, the model emits spike early after this perturbation. Figure 4a also illustrates the behaviour of the model if no perturbation was given. The negative and different amplitude perturbation is given at the different time point as shown in Figure 4b. At the 45.5<sup>th</sup>ms-14 pA square pulse current applied to oscillator during 0.8 ms. As shown in this figure, the period of oscillation changed very slightly with this perturbation. The voltage-time graph zooms in at the insert. Figure 4c shows limit cycle attractor, the initial condition of the oscillator and applied perturbation point of the negative amplitude current, -14 pA, in more detail.

Although direct method (see Eq. (4)) is a simple method, this method is not exactly correct.<sup>53</sup> Since the magnitude and duration of applied current could change or different for varied oscillators and these are important factors which directly change shape of PRCs.

## 2.5. Linear adjoint method

The used neural model is composed of two equations, Eq. (1a) and Eq. (1b), the detailed description mentioned above. These two equations imply 2-dimensional state

space  $X = (X_v, X_n)$ . The  $I_{Na,p} + I_K$  model can be written as follow,

$$\frac{d}{dt}X = F(X) \quad (5)$$

Assume that this system moves on stable limit cycle attractor with a period of  $T$ . The angular velocity of this system is  $w=2\pi/T$  and  $X_0(t+T) = X_0(t)$ . The phases of points in the limit cycle can be converted to the length of limit cycle, angle and time. If the phases of points are converted to time mode, the phase of any point on limit cycle is written as

$$\theta = wt \pmod{2\pi}, \text{ and } \theta(t) \in [0, 2\pi) \quad (6)$$

At Eq. (6),  $\theta$  represents the phase of point,  $w$  implies angular velocity, and  $t$  represents time. It is also possible to find phases of the point which are not on limit cycle but attract it with time. The small perturbation given to limit cycle attractor which generates the basis of PRC is given by

$$\frac{d}{dt}X = F(X) + \varepsilon P(t) \quad (7)$$

At Eq. (7),  $P(t)$  represents small perturbation. Eq. (8a) represents phase model of weakly connected oscillators. Phase deviation is given by  $\varphi$  and the period of oscillations is the same for all oscillators.<sup>2</sup> Eq. (8b) represents time derivative of phase model given in Eq. (8a).

$$\theta(t) = t + \varphi(t) \quad (8a)$$

$$\dot{\theta}(t) = 1 + \dot{\varphi}(t) \quad (8b)$$

Eq. (9) shows the parameters related to the derivative of phase deviation. In this equation,  $P(t)$  implies small amplitude perturbation,  $Q(\theta)$  represents phase response curve, in other words,  $Q(\theta)$  implies the sensitivity of phase of  $\theta(t)$  to perturbation  $P(t)$ .<sup>54</sup>

$$\dot{\varphi}(t) = Q(\theta(t))P(t) \quad (9)$$

If the value of Eq. (9) is written in Eq. (8b), Eq. (10) is obtained.

$$\dot{\theta}(t) = 1 + Q(\theta(t))P(t) \quad (10)$$

At this equation,  $Q$  is a solution of linear adjoint equation with a function of  $T$ -period.

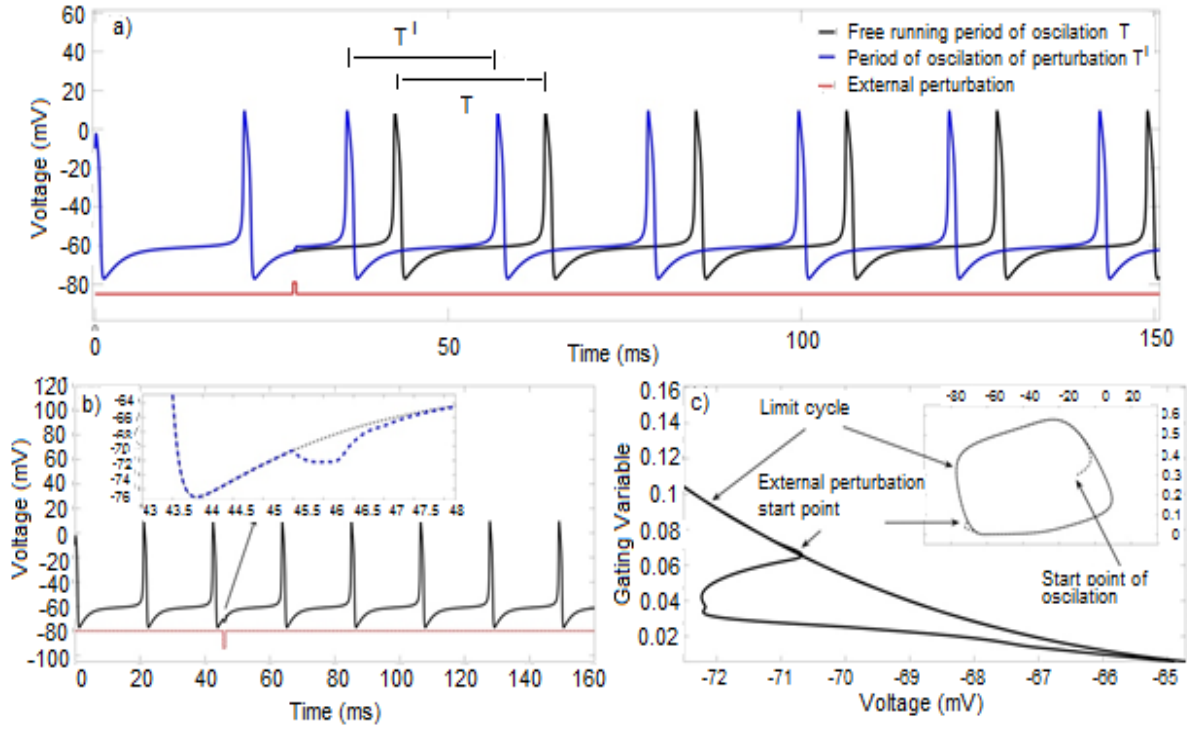


**Figure 4.** Voltage-time graph of the neuron model: a) Positive stimulus, b) Negative stimulus, c) Change of limit cycle.

At Eq. (11a),  $\{DF(X(t))\}^T$  is the transposed Jacobian matrix of function F on the limit cycle attractor at the point  $X(t)$ . Eq. (11b) represents the initial condition of the system.

$$\dot{Q} = -\{DF(X(t))\}^T Q \quad (11a)$$

$$Q(0) \cdot F(X(0)) = 1 \quad (11b)$$

Adjoint method has centered on Malkin's approach.<sup>55</sup> Calculated PRC must be periodic, i.e.  $Q(T)=Q(0)$ , because of this reason, the direct integration of this equation is not suitable due to boundary value problem.<sup>53</sup> To find the periodic solution of Eq. (11a) is integrated backward in time.<sup>32,56</sup> The proof of adjoint equation<sup>55</sup> and invaluable studies for obtaining PRC are available at the selected papers.<sup>2,14,57</sup>

### 2.6. Adapted direct method

Adapted Direct Method proposed by Noviĉenko and Pyragas was tested for different neural models. The results of these tests show that adapted directed method

up to 10 to 100 times faster than linear adjoint method.<sup>53</sup> Although linear adjoint method getting very slow at the situation when the limit cycle is near to bifurcation point, the speed of adapted direct method does not depend on it. Adapted direct method described by

$$PRC(\theta) = \frac{L_1(\theta)}{L_1^T(\theta)V(\theta)} \quad (12)$$

At Eq. (12),  $L_1$  is left eigenvector, and  $V(\theta)$  is equal to the velocity vector. The detailed proof of this method can be found from Noviĉenko study.<sup>53</sup> PRC is calculated by using this method by means of the Viktor Noviĉenko software code. So, the computation of PRC is done numerically by the help of this software code.<sup>58</sup>

### 3. RESULTS

The PRCs of  $I_{Na,p} + I_K$  model were calculated by the help of three different methods and the results are given in Figure 5. The PRCs calculated by using direct method, linear adjoint method and adapted direct method are illustrated in Figure5a-c, respectively. Although the shapes of numerically calculated PRCs were similar to

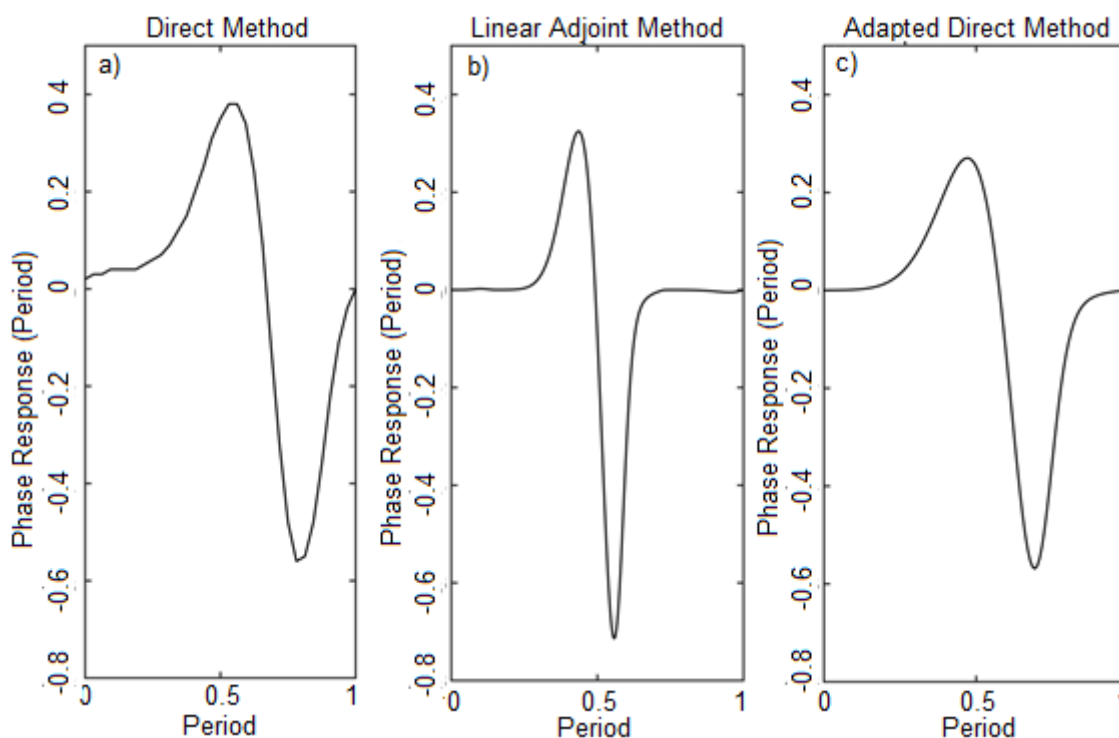


**Figure 5.** Phase response curves: a) Direct method, b) Linear adjoint method, c) Adapted direct method.

each other's, they were not exactly the same. The calculated phase response values of direct method are approximately ten times smaller than the other methods. The magnitude of the early and late peak of PRC was biggest at the linear adjoint method. These PRCs were calculated by using Type-2 excitability parameters (Table 1), and 35 pA external current applied.

The results of early and late peaks, peak-to-baseline ratios and required time intervals are given in Table 2 for these three methods. The required simulation time for direct method was approximately 190 times longer than adapted direct method and 40 times longer than linear adjoint methods. This means that the PRC computation speed is fastest at the adapted direct method and the slowest calculation speed is at the direct method. Linear adjoint method and adapted direct method gave similar results considering to the peak-to-baseline ratio. It is assumed that the reason of varied peak to baseline ratio at the direct method is due to the fact that the magnitude and duration of perturbations are not standard at this model. To conclude that, in this study, at first, excitability types and their corresponding phase response curves were derived for  $I_{Na,p} + I_K$  model. The peak to baseline ratio is mentioned. After then, PRC of  $I_{Na,p} + I_K$  model were calculated by using direct method, linear adjoint method and adapted direct method. The results of these three different methods were compared in terms of simulation speed and peak to baseline ratios.

**Table 2.** The peak-to-baseline ratios and simulation times for the PRCs derived for Type-2 excitability of  $I_{Na,p} + I_K$  model

	Direct method	Linear adjoint method	Adapted direct method
$m_e$	0.038	0.325	0.270
$m_l$	-0.056	-0.708	-0.569
Peak-to-baseline ratio( $r$ )	5.22	2.697	2.806
Required time interval (s)	107.85	2.75	0.56

This study can enlighten how to calculate PRC in terms of three different methods and gives the idea about advantage and disadvantage of these methods.

#### ACKNOWLEDGEMENT

Authors thank to Kahramanmaraş Sütçü İmam University for continuous motivation. Hasan ESKALEN thanks to Scientific and Technological Research Council of Turkey (TUBITAK) for Ph.D. scholarship (2211-C Program).

**Conflict of interest**

We declare that there is no a conflict of interest with any person, institute, and company, etc.

**REFERENCES**

- Hodgkin, A.L.; Huxley, A. F. *J. Physiol.* **1952**, 117 (4), 500-544.
- Izhikevich, E.M. *Dynamical systems in Neuroscience*, MIT press: 2007.
- Rich, S.; Booth, V.; Zochowski, M. *Front. Neural Circuits* **2016**, 10, 82.
- Park, Y.; Ermentrout, B. *J. Comput. Neurosci.* **2016**, 40 (3), 269-281.
- Van Der Pol, B.; Van Der Mark, J. *The London, Edinburgh, and Dublin Phil. Mag. J. Sci.* **1928**, 6 (38), 763-775.
- Kralemann, B.; Frühwirth, M.; Pikovsky, A.; Rosenblum, M.; Kenner, T.; Schaefer, J.; Moser, M. *Nat. Commun.* **2013**, 4, 3418.
- Funato, T.; Yamamoto, Y.; Aoi, S.; Imai, T.; Aoyagi, T.; Tomita, N.; Tsuchiya, K. *PLoS Comput. Biol.* **2016**, 12 (5), e1004950.
- Nessler, J.A.; Spargo, T.; Craig-Jones, A.; Milton, J.G. *Gait Posture* **2016**, 43, 187-191.
- Minors, D. S.; Waterhouse, J. M.; Wirz-Justice, A. *Neurosci. Lett.* **1991**, 133 (1), 36-40.
- Eck, S.; Helfrich-Förster, C.; Rieger, D. *J. Biol. Rhythm.* **2016**, 31 (5), 428-442.
- Field, R. J.; Noyes, R. M. *J. Chem. Phys.* 1974, 60 (5), 1877-1884.
- Proskurkin, I.S.; Vanag, V.K., *Phys. Chem. Chem. Phys.* **2015**, 17 (27), 17906-17913.
- Franović, I.; Kostić, S.; Perc, M.; Klinshov, V.; Nekorkin, V.; Kurths, J. *Chaos* **2016**, 26 (6), 063105.
- Nakao, H. *Contemp. Phys.* **2016**, 57 (2), 188-214.
- Pikovsky, A.; Rosenblum, M.; Kurths, J. *Synchronization: a universal concept in nonlinear sciences*. Cambridge University Press: 2003; Vol. 12.
- Strogatz, S.H. *Nonlinear dynamics and chaos: with applications to physics, biology, chemistry, and engineering*. Hachette UK: 2014.
- Smeal, R.M.; Ermentrout, G.B.; White, J.A. *Philos. Trans. R. Soc. Lond. B: Biol. Sci.* **2010**, 365 (1551), 2407-2422.
- Stein, R. *Proceedings of the Royal Society of London B: Biological Sciences* 167 (1006), 64-86, 1967.
- Tateno, T.; Harsch, A.; Robinson, H. *J. Neurophysiol.* **2004**, 92 (4), 2283-2294.
- Uhlhaas, P. J.; Singer, W. *Neuron* **2006**, 52 (1), 155-168.
- Spencer, K.M.; Nestor, P.G.; Perlmutter, R.; Niznikiewicz, M.A.; Klump, M.C.; Frumin, M.; Shenton, M.E.; McCarley, R.W. *Proceedings of the National Academy of Sciences of the United States of America* 101 (49), 17288-17293, 2004.
- Uhlhaas, P.J.; Linden, D.E.; Singer, W.; Haenschel, C.; Lindner, M.; Maurer, K.; Rodriguez, E. *J. Neurosci.* **2006**, 26 (31), 8168-8175.
- Krishnan, G.P.; Vohs, J.L.; Hetrick, W.P.; Carroll, C. A.; Shekhar, A.; Bockbrader, M. A.; O'Donnell, B.F. *Clin. Neurophysiol.* **2005**, 116 (3), 614-624.
- Stam, C.J.; Jones, B.; Nolte, G.; Breakspear, M.; Scheltens, P. *Cereb. Cortex* **2006**, 17 (1), 92-99.
- König, T.; Prichep, L.; Dierks, T.; Hubl, D.; Wahlund, L.; John, E.; Jelic, V. *Neurobiol. Aging* **2005**, 26 (2), 165-171.
- Hammond, C.; Bergman, H.; Brown, P. *Trends Neurosci.* **2007**, 30 (7), 357-364.
- Schnitzler, A.; Gross, J., *Nat. Rev. Neurosci.* **2005**, 6 (4), 285-296.
- Holt, A.B.; Wilson, D.; Shinn, M.; Moehlis, J.; Netoff, T.I. *PLoS Computat. Biol.* **2016**, 12 (7), e1005011.
- Milton, J. G. *Epilepsy Behav.* **2010**, 18 (1), 33-44.
- Bressloff, P. C.; Ermentrout, B.; Faueras, O.; Thomas, P. J. *J. Math. Neurosci.* **2016**, 6 (4), 1-9.
- Delaunay, F. *B. Cancer* **2017**, 104 (10), 821-822.
- Ermentrout, B. *Neural Comput.* **1996**, 8 (5), 979-1001.
- Brown, E.; Moehlis, J.; Holmes, P. *Neural Comput.* **2004**, 16 (4), 673-715.
- Marella, S.; Ermentrout, G.B. *Phys. Rev. E*, **2008**, 77 (4), 041918.

35. Ermentrout, G. B.; Galán, R. F.; Urban, N. N. *Trends Neurosci.* **2008**, 31 (8), 428-434.
36. Qiao, W.; Wen, J. T.; Julius, A. *IEEE T. Automat. Contr.* **2017**, 62 (1), 445-450.
37. Sato, Y. D.; Aihara, K. *Neural Comput.* **2014**, 26 (11), 2395-2418.
38. Canavier, C. C. *Curr. Opin. Neurobiol.* **2015**, 31, 206-213.
39. Buchin, A.; Rieubland, S.; Häusser, M.; Gutkin, B. S.; Roth, A. *PLoS Comput. Biol.* **2016**, 12(8), e1005000.
40. Cui, J.; Canavier, C.C.; Butera, R.J. *J. Neurophysiol.* **2009**, 102 (1), 387-398.
41. Tateno, T.; Robinson, H. *Biophys. J.* **2007**, 92 (2), 683-695.
42. Galán, R.F.; Ermentrout, G.B.; Urban, N.N. *Phys. Rev. Lett.* **2005**, 94 (15), 158101.
43. Saifee, T.A.; Edwards, M.J.; Kassavetis, P.; Gilbertson, T. *J. Neurophysiol.* **2015**, 115 (1), 310-323.
44. Jones, J. R.; Tackenberg, M. C.; McMahon, D.G. *Nat. Neurosci.* **2015**, 18 (3), 373-375.
45. Ostojic, S.; Szapiro, G.; Schwartz, E.; Barbour, B.; Brunel, N.; Hakim, V. *J. Neurosci.* **2015**, 35 (18), 7056-7068.
46. Miranda-Dominguez, O.; Netoff, T.I. *J. Neurophysiol.* **2013**, 109 (9), 2306-2316.
47. Kobelevskiy, I. Bifurcation analysis of a system of Morris-Lecar neurons with time delayed gap junctional coupling. Mater Thesis, University of Waterloo, 2008.
48. Izhikevich, E.M. *IEEE T. Neural Networ.* **1999**, 10 (3), 499-507.
49. Izhikevich, E.M. *Int. J. Bifurcat. Chaos* **2000**, 10 (06), 1171-1266.
50. Yu, T.; Sejnowski, T. J.; Cauwenberghs, G. *IEEE T. Biomed. Circ. S.* **2011**, 5 (5), 420-429.
51. Phoka, E.; Cuntz, H.; Roth, A.; Häusser, M. *PLoS Computat. Biol.* **2010**, 6 (4), e1000768.
52. Couto, J.; Linaro, D.; De Schutter, E.; Giugliano, M. *PLoS Comput. Biol.* **2015**, 11 (3), e1004112.
53. Novičenko, V.; Pyragas, K. *Nonlinear Dynam.* **2012**, 67 (1), 517-526.
54. Fang, Y.; Yashin, V. V.; Jennings, B. B.; Chiarulli, D. M.; Levitan, S. P. *ACM J. Emerg. Tech. Com.* **2016**, 13 (2), 14.
55. Hoppensteadt, F. C.; Izhikevich, E.M. *Weakly connected neural networks*. Springer Science & Business Media: 2012; Vol. 126.
56. Ermentrout, B. *Simulating, analyzing, and animating dynamical systems: a guide to XPPAUT for researchers and students*. Book Code: SE14, SIAM, 2002.
57. Nakao, H.; Yanagita, T.; Kawamura, Y. *Phys. Rev. X*, **2014**, 4, 021032 (1-23).
58. Novičenko V webpage. <http://www.itpa.lt/~novicenko/index.php?page=soft> (accessed June 14, 2017).

 ORCID

 0000-0002-4523-6573 (H. Eskalen)

 0000-0001-9334-327X (Ş. Özğan)